Research Square

Preprints are preliminary reports that have not undergone peer review.
They should not be considered conclusive, used to inform clinical practice,
or referenced by the media as validated information.

MicroRNA-381 inhibits bladder cancer pathogenesis through directly controlling BMI1 and triggering the Rho/ROCK signaling pathway defect

Dayin Chen
the Fisrt Affiliated Hospital of Jiamusi University
Liang Cheng
the First Affiliated Hospital of Jiamusi University
Huifeng Cao (huifengG010601@163.com)
the First Affiliated Hospital of Jiamusi University https://orcid.org/0000-0002-6199-3814
Wensi Liu
the First Affiliated Hospital of Jiamusi University

Research article

Keywords: miR-381, BMI1, Rho/ROCK signaling pathway, Bladder cancer, Microarray analysis

Posted Date: May 4th, 2020

DOI: https://doi.org/10.21203/rs.3.rs-23467/v1

License: This work is licensed under a Creative Commons Attribution 4.0 International License.
Read Full License

Version of Record: A version of this preprint was published on January 6th, 2021. See the published version at https://doi.org/10.1186/s12894-020-00775-3.

Abstract

Background

Emerging evidence has noted the important participation of microRNAs (miRNAs) in several human diseases including cancer control. This research was launched to probe the function of miR-381 in bladder cancer (BCs) progression.

Methods

Aberrantly expressed miRNAs in BCs tissues were analyzed using miRNA microarrays. miR-381 expression in the bladder and paired tumor tissues, and in BCs and normal cell lines was determined. The target relationship between miR-381 and BMI1 was predicted online and validated through a luciferase assay. Gain-of-functions of miR-381 and BMI1 were performed to identify their functions on BCs cell behaviors as well as tumor growth *in vivo*.

Results

miR-381 was poor regulated in BCs tissues and cells. A higher miR-381 level indicates a better prognosis of patients with BCs. Artificial up-regulation of miR-381 inhibited proliferation, invasion, migration, resistance to apoptosis, and tumor formation ability of BCs cells. miR-381 directly binds to BMI1 expression. Overexpression of BMI1 partially blocked the tumor suppressing roles of miR-381 in cell malignancy and tumor growth. In addition, miR-381 led to decreased RhoA phosphorylation and ROCK2 activation, which were also reversed by BMI1.

Conclusion

The study evidenced that miR-381 may act as a beneficiary biomarker in BCs patients. Up-regulation of miR-381 could suppress BCs development both in vivo and in vitro through BMI1 down-regulation and the Rho/ROCK inactivation.

Background

Cancer is a major public health concern across the globe, and the urinary bladder cancer (BCs) is the most common neoplastic diseases in the urinary system with 81400 estimated cases in 2020 in the United States alone according to the up-to-date Cancer Statistics [1]. Nearly 165,000 cases die from this malignancy around the world every year, and males have a 3-fold predominance in morbidity against females, possibly because of the long-term smoking prevalence and exposure to occupational carcinogens [2]. BCs is allocated to two important branches according to the disease states, which are non-muscle invasive BCs (NMIBD, < T2 stage) and the more risky and metastatic type, muscle invasive

BCs (MIBD, T2-T4 stage) with the current or future distant invasion potential [3]. However, tumor recurrence is a major challenge of the BCs treatment with a rate of 61% in the first year, and the approximately 3%-15% recurrent NMIBD may progress to the invasive type MIBD when obtaining additional genetic mutations [4]. The current treatment for BCs is far below expectations, with the survival rate of patients saw little improvement during the last decades [2]. Identifying more molecular mechanisms may help develop novel effective treatments for this disease.

MicroRNAs (miRNAs), a large family of non-coding RNAs with 22 nucleotides in length, regulate multiple biological processes and are aberrantly expressed in human diseases including cancers [5]. miRNAs are well-known to exert key functions by inducing complementary target mRNA repression post-transcriptionally through the 3'untranslated region (3'UTR) [6]. Here in the paper, the miRNA microarray analysis was performed with miR-381 found as a major down-regulated miRNA in the BCs tissues. miR-381 has been noted as a tumor inhibitor in many human cancers [7, 8]. In addition, it is noteworthy that miR-381-3p may inhibit CDK6 and MET-mediated epithelial-mesenchymal transition (EMT) and cell cycle progression of BCs cells [9]. But the roles of miR-381 in BCs progression are far away from being fully researched. Here, our study identified BMI1 as a putative mRNA target of miR-381. BMI1 is a key protein of polycomb repressive complex 1 that functions in integrity maintenance, and it has been increasingly known as a factor in the development of multiple human cancers [10]. Thereby, we proposed that miR-381 inhibits malignant behaviors of BCs through the down-regulation of BMI1. Altered expression of miR-381 and BMI1 was induced to explore their roles in cell malignant behaviors as well as the tumor growth *in vivo*, and the potential downstream signaling pathway was identified.

Methods

Clinical sample collection

BCs tissues and the paired adjacent tissues were obtained from 28 BCs patients (22 males and 6 females) who admitted into the First Affiliated Hospital of Jiamusi University from January 2013 to January 2015 with a mean age of 65 ± 5.67 years. A 4-year follow-up study was performed to record the prognosis of patients at a 3-month interval. The patients were divided into T1 to T4 stages according to the Tumor-Node-Metastasis (TNM) staging, with 7 in T1, 13 in T2, 5 in T3, and 3 in T4. All included patients had neither pre-surgery treatment history nor chemoradiotherapy history, and they were pathologically diagnosed as primary BCs free of other diseases. The tumor tissues and the adjacent tissues (at least 3 cm away from the tumor tissues) were resected during surgery and preserved in liquid nitrogen. The demographic characteristics of the respondents are exhibited in Table 1.

Table 1
Clinical feature of included patients

Item	Group	n
Gender	Male	22
	Female	6
Age	≤ 60	5
	> 60	23
TNM stage	T1	7
	T2	13
	T3	5
	T4	3
History of smoking	yes	25
	no	17
Note: TNM, Tumor Node Metastasis.		

miRNA microarray analysis

Four patients in T1, T2, T3 or T4 stage (one in each stage) were enrolled for miRNA microarray analysis. The tumor and the paired adjacent tissues from patients were collected for total RNA extraction using TRIzol Reagent (Invitrogen, Carlsbad, CA, USA). Total RNA was concentrated in isopropanol, and then the RNA purity was detected using NanoDrop 2000C (Thermo Fisher Scientific Inc., Waltham, MA, USA) and the RNA quality was determined by formaldehyde denatured agarose gel electrophoresis. Then, 50 μg total RNA was purified using a Taqman miRNA ABC purification kit (Thermo Fisher) and hybridized with the beads. The beads were then washed with magnet, and the miRNAs were eluted 3 times to collect the miRNAs. Thereafter, the collected miRNAs were labeled using a miRNA Complete Labeling and Hyb Kit (Agilent, USA). In brief, 100 μg total RNA was incubated in 10 μg Labeling Spike-In at 37℃ for 30 minutes, treated with DMSO at 16℃ for 2 hours, dried in a vacuum concentrator at 45℃ for 3 hours, and then treated with Hybridization Mixture and Hyb labeling at 55℃ for 20 hours for hybridization. Then, the miRNAs were further hybridized with Human miRNA Microarray Release 14.0,8 (Agilent, USA) and scanned using a SureScan Dx Microarray Scanner (Agilent, USA). The obtained data were subjected to Quality Center analysis and normalization to produce the heatmap for differentially expressed miRNAs.

Reverse transcription quantitative polymerase chain reaction (RT-qPCR)

Total RNA for cells or tissues was extracted using TRIzol Reagent and reversely transcribed into cDNA using a PromeScript^{TM}RT Master Mix Kit (Takara Bio, Jan) and amplified. Relative gene expression was

quantitated using a SYBR®Premix Ex Taq™II Kit (Takara Bio, Jan). The qPCR was performed on a Mx3005P System (Stratagene, USA). Quantification of each sample was repeated by three times. Relative expression was evaluated using the $2^{-\Delta\Delta Ct}$ method with U6 and GAPDH as internal references. Table 2 exhibits the primer sequences.

Table 2
Primer sequences for RT-qPCR

Gene	Primer sequence (5'-3')
miR-381	F: TATACAAGGGCAAGCTCUCTGT
	R: TGCGGGTGCTCGCTTCGGCAGC3
BMI1	F: TGGATCGGAAAGTAAACAAAGAC
	R: TGCATCACAGTCATTGCTGCT
GAPDH	F: GGGAGCCAAAAGGGTCATCA
	R: TGATGGCATGGACTGTGGTC
U6	F: CTCGCTTCGGCAGCACA
	R: AACGCTTCACGAATTTGCGT

Cell culture and transfection

Human bladder cell lines T24 and RT4, normal bladder epithelial cell line SV-HUC-1, and HEK-293T cells were acquired from ATCC (Manassas, USA). Cells were cultivated in Dulbecco's modified Eagle's medium with 10% fetal bovine serum (FBS, all from Gibco Company, Grand Island, NY, USA) at 37℃ with 5% CO_2. The miR-381 mimic and BMI1-overexpressing vectors (BMI1-OE) were synthesized by GenePharma Co., Ltd. (Shanghai, China). To minimize the off-target effects, 3 RNA fragments were loaded into the vectors and transfected into cells. Then cells were plated into 24-well plates once the cell confluence reaching 70%. miR-381 mimic and BMI1-OE vectors were transfected into T24 and RT4 cells in line with the protocols of the Lipofectamine 2000 (Invitrogen). After 6 hours, the fluorescence expression in cells was observed under a fluorescence microscope (Olympus Optical Co., Ltd, Tokyo, Japan)

Cell proliferation by the Cell Counting Kit-8 (CCK-8) method

A total of 100 μL cell suspension was loaded on 96-well plates and pre-incubated for 24 hours. Next, each well was loaded with 10 μL CCK-8 reagent, and then the plates with cells were further incubated for 12, 24, 48 and 72 hours. Then the optical density at 450 nm was evaluated using a microplate reader (SoectraMax iD5, Molecular Devices, USA). The CCK-8 kit was from Dojindo Laboratories (Kumamoto, Japan).

Cell migration by scratch test

Guide lines were produced on the back side of 6-well plates at a 1-cm interval, and 5×10^5 cells were added into the plates. On the second day, a pipette was used to produce a scratch perpendicular to the back side guide lines, and the scratched cells were washed away by phosphate buffer saline (PBS). Then the plates were loaded with serum-free medium and cultured at 37℃ with 5% CO_2. Twenty-four hours later, the cells were observed and photographed under a microscope (CX22, Olympus). The scratch area was analyzed using the Image J software (version 1.48, NIH, USA). Relative migration distance (%) = (0 h scratch area − 24 h scratch area)/0 h scratch area [11].

Cell invasion by transwell assay

Matrigel was diluted in serum-free DMEM, and then 100 μL Matrigel was loaded onto each apical chamber at 37℃ for 4 hours. Then, cells were resuspended in 10% FBS to 5×10^5 cells/mL, and each apical chamber was loaded with 200 μL cell suspension, while each basolateral chamber was loaded with 600 μL cell medium (containing 5 μg/mL fibronectin). Then transwells were incubated at 37℃ for 20 hours, and the non-invaded cells in the apical chambers were removed, while the invaded cells in each well were stained with 500 μL 0.1% crystal violet at 37℃ for 30 minutes. Then the number of invaded cells were observed and counted under the microscope with 5 random fields included.

Flow cytometry

In short, 27 mL ddH_2O was used to dilute 3 mL Binding Buffer (10 ×), and cells in each group were resuspended in 1 mL 1 × Binding Buffer, centrifuged at 300 g for 10 min to discard the supernatant, and resuspended in 1 mL 1 × Binding Buffer again till a density of 1×10^6 cells/mL. Next, each tube was loaded with 100 μL cells and then 5 μL Annexin V-fluorescein isothiocyanate (FITC) for 10 min of reaction, and then with 5 μL propidium iodide (PI) in the dark for 5 min. The apoptosis was determined using an Annexin V-FITC/PI Apoptosis Kit (Solarbio Science & Technology Co., Ltd., Beijing, China) and run on a flow cytometer (Attune Nxt, Thermo Fisher) within an hour.

Xenograft tumors in nude mice

A total of 48 specific-pathogen-free nude mice (4–6 weeks old, 20 ± 2 g) purchased from Vital River Laboratory Animal Technology Co., Ltd. (Beijing, China) were randomly allocated into 6 groups, 8 in each. Then, each mouse was subcutaneously injected with 4×10^6 T24 or RT4 cells with stable miR-381 mimic or mimic control transfection, or cells with BMI1-OE and vector control transfection. The volume (V) of xenograft tumors was calculated as the following formula every 7 days: $V = (L \times W^2)/2$, where 'L' indicates the length while 'W' indicates the width [12]. On the 28th day after cell implantation, mice were euthanized by overdose of pentobarbital sodium (150 mg/kg), and the tumors were taken out and weighed.

Dual-luciferase reporter gene assay

The binding relationship between miRNA and mRNA was predicted on StarBase (http://starbase.sysu.edu.cn/). The 3'UTR sequence of BMI2 and miR-381 was inserted into pMIR-REPORT™ luciferase reporter vector (Thermo Fisher) using Lipofectamine 3000 (Invitrogen) and then

transfected into HEK293T cells. Cells were lysed 24 hours later, and the luciferase activity was determined using a Dual-Luciferase Reporter Assay System (Promega Corporation, WI, USA) [13]. Three independent experiments were performed.

Western blot analysis

Radio-Immunoprecipitation assay cell lysis buffer (Amresco Inc., Texus, USA) was used to collect total protein, which was then and centrifuged at 800 g at 4℃ for 5 min to collect the cells. Then the cells were ice-bated in a 5-fold volume of lysis buffer for 10 min, and then centrifuged at 12,000 g at 4℃ for 10 min to collect the supernatant. The protein was run on SDS-PAGE and transferred to polyvinylidene fluoride membranes (EMD Millipore). Subsequently, the membranes were blocked with 5% skimmed milk and then incubated with the primary antibodies against RhoA (1:5000, ab187027), p-RhoA (1:1000, ab41435), ROCK2 (1:5000, ab71598) and β-actin (1:1000, ab8227) (Abcam Inc., Cambridge, MA, USA) at 4℃ for 16 hours, and then with the secondary antibody (1:3000, ab205718) at room temperature for 2 hours. The immunoblotting image were visualized using the Image J software (Version 1.8.0, National Institute of Health, USA). Three independent experiments were performed.

Statistical analysis

SPSS 22.0 (IBM Corp. Armonk, NY, USA) was used for data analysis. Data were in normal distribution according to Kolmogorov-SmiRnov test and are exhibited as mean ± standard deviation (mean ± SD). Differences in multiple groups were analyzed using one-way or two-way analysis of variance (ANOVA). Tukey's multiple comparisons test was used for the post-hoc test after ANOVA analysis. Survival curve was drawn using the Kalpan-Meier method and analyzed using the log rank test. p was obtained by two-tailed tests and $p < 0.05$ was regarded statistically significant.

Results

Poor miR-381 expression in BCs patients indicates unfavorable prognosis

The tumor tissues and paired adjacent tissues from 4 BCs patients (T1 to T4) were used for miRNA microarray analysis. It was found that miR-381 was the greatest down-regulated one in tumor tissues as compared to the normal tissues (Fig. 1A). Then, the RT-qPCR results validated that miR-381 was significantly poorly expressed in the tumor tissues in all the included BCs patients (Fig. 1B). According to the average miR-381 expression (0.46), the patients were allocated into high-expression group (n = 16) and low-expression group (n = 12). The follow-up study data suggested that patients with higher miR-381 had relatively higher survival rates and longer lifetime (Fig. 1C). In addition, we also determined miR-381 expression in cell levels, and it was noteworthy that miR-381 expression was much lower in BCs cell lines T24 and RT4 than that in normal bladder epithelial cells (Fig. 1D).

miR-381 inhibits malignant behaviors of BCs cells

To further figure out the roles of miR-381 in BCs development, up-regulation of miR-381 was introduced in both T24 and RT4 cell lines by administrating miR-381 mimic or mimic control (Fig. 2A). Then, we found that miR-381 mimic treatment led to a significant decline in proliferation in both cells (Fig. 2B). Accordingly, cells with increased miR-381 expression presented decreased migration distance (Fig. 2C) and reduced number of invaded cells (Fig. 2D). In addition, it was found that miR-381 mimic led to increased cell apoptosis (Fig. 2E). As for *in vivo* experiments, the implantation of cells with miR-381 mimic led to a significant decline in tumor growth in mice, and the tumor weight was decreased on the 28th day (n = 8) (Fig. 2F).

miR-381 targets BMI1 to inactivate the Rho/Rock pathway

We next explored the potential downstream molecules involved. We first predicted BMI1 as a target of miR-381 on a computer-based bioinformation system, and then had the binding relationship between miR-381 and BMI1 validated through a luciferase assay (Fig. 3A). Then, it was found that BMI1 expression was increased in tumor tissues as compared to the adjacent tissues (Fig. 3B), and similarly, the BMI1 expression was also higher in BCs cell lines than that in bladder epithelial cells (Fig. 3C). The BMI1 expression in the tumor tissues of BCs patients was negatively correlated with miR-381 expression (Fig. 3D). BMI1-OE vectors were administrated into T24 cells and RT4 cells, and BMI1-OE#2 presented a best overexpressing efficiency (Fig. 3E). After miR-381 control, miR-381 mimic, BMI1-NC or BMI1-OE vector transfection, the protein levels of RhoA and ROCK2 were detected. It was found that miR-381 mimic inhibited the phosphorylation of RhoA and ROCK2 while BMI1-OE led to increased activation of the Rho/ROCK signaling pathway (Fig. 3F). The above results indicated that miR-381 could target BMI1 to inactivate the Rho/Rock pathway.

Overexpression of BMI1 promotes BCs progression

To further identify the exact roles of BMI1 in BCs pathogenesis, overexpression of BMI1 was artificially up-regulated in T24 and RT4 cells. BMI1-OE vector led to an increase in cell proliferation (Fig. 4A). Likewise, the migration rate (Fig. 4B) and invasion rate (Fig. 4C) of cells was notably increased following BMI1 overexpression. In addition, overexpression of BMI1 reduced the apoptosis rate in both cell lines (Fig. 4D). As for *in vivo*, we found cells transfected with BMI1-OE led to significantly increased tumor growth rate and weight in nude mice (n = 8) (Fig. 4E). These results identified BMI1 presented a reverse regulating role in BCs cells as relative to miR-381.

BMI1 partially blocks the role of miR-381

To further confirm the involvement of BMI1 in the miR-381-mediated events. Overexpression of BMI1 was introduced in cells pre-transfected with miR-381 mimic (Fig. 5A). It was found that further overexpression of BMI1 partially recovered cell proliferation (Fig. 5B), cell migration (Fig. 5C) and cell invasion (Fig. 5D) that was suppressed by miR-381 mimic. In addition, the miR-381-triggerred cell apoptosis was inhibited when BMI1 was further overexpressed (Fig. 5E). Accordingly, cells transfected miR-381 mimic and BMI-OE

vector led to an increased tumor growth rate in nude mice compared to cells with miR-381 mimic alone (Fig. 5F). These findings suggested that BMI1 partially antagonized the effects of miR-381 mimic.

Discussion

Treatment for BCs, especially for the invasive type MIDB remains great challenge owing to high recurrence following surgical resection and drug administration. Aside from the unfavorable prognosis, the huge economic cost in lifetime surveillance with periodic cystoscopy and evaluation of recurrence rate brings considerable burden to BCs patients [14–16]. It has been as an emerging consensus that aberrant expression of some miRNAs, either extremely high or poor expression, is closely correlated with BCs pathogenesis [17]. Here, the current study evidenced that miR-381 could serve as a cancer suppressor in BCs with the involvement of BMI1 downregulation and the following Rho/ROCK inactivation.

The initial finding was that miR-381 was poorly expressed in the tumor tissues in BCs patients and was positively correlated with patient prognosis, preliminarily indicating a beneficiary role of miR-381 in BCs prognosis. miRNAs have been emerged as non-invasive biomarkers for BCs detection [18, 19] or even potential treating targets in clinical practice [20]. For instance, miR-3622a was noted to promote proliferation and invasion capacities of BCss through binding to LASS2 [11]. On the other hand, some miRNAs have been documented to exert suppressing functions in BCs. miR-502-5p, for example, has been recently found to suppress the malignant behaviors of BCs cells through the different miRNA targets including CCND1, NOP14 and DNMT3B [21]. Similar trends have also been previously in miR-124-3p [22] and miR-203a [23]. As for miR-381, it has been particularly suggested to play critical functions in overcoming cisplatin resistance in breast cancer treatment [24–26]. Likewise, its anti-tumor role has been increasingly revealed in other malignancies such as in cervical cancer [27] and in prostate cancer [28] through the different mRNA targets. Here our study found that miR-381 was poorly expressed in BCs cells. Overexpression of miR-381 inhibited the malignant behaviors of BCs T24 and RT4 cell lines, presenting as decreased cell viability, reduced cell migration and invasion, and increased cell apoptosis. In addition, similar results were found in animal experiments, where cells with stable miR-381 overexpression contributed to a significant inhibition in tumor growth in volume and weight regards.

Second, the findings above triggered us to further explore the downstream molecules of miR-381. A computer-based online prediction system suggested BMI1 as a target mRNA of miR-381, and this binding relationship was further validated by a luciferase assay. As a member of the polycomb group family, BMI1, owning stem cell characteristics, is prone to participate in the onset and development of tumors and is linked to tumor metastasis, recurrence and chemo-resistance as well [29]. In addition, BMI1 is well-known to interact with another EMT and stemness promoter, TWIST1 [30, 31]. Not surprisingly, silencing of BMI1 has been suggested as a promising therapeutic target in many human cancer therapies [32, 33]. Here, our study found that artificial overexpression of BMI1 led to increased cell proliferation, migration, invasion and resistance to death in both T24 and RT4 cells. The involvement of BMI1 in BCs pathogenesis has been relatively largely studied. Its knockdown was noted to inhibit bladder cell growth,

self-renewal and progression, and several upstream mediators of BMI1 such as miR-139-5p [34] and miR-200c [35] were identified. In the current paper, in order to further validate that BMI1 silencing holds accountable for the miR-381-mediated events, rescue experiments were performed where cells pre-transfected with miR-381. It was found that the malignant behaviors of cells inhibited by miR-381 mimic was partially recovered following BMI1 overexpression.

The Rho/ROCK signaling is well-known for its implication in cytoskeletal reorganization, which is elemental for cell migration and metastasis [36]. Here, our study identified that the phosphorylation of RhoA and ROCK2 expression was notably inhibited by miR-381, while overexpression of BMI1, notably, led to reversed trends. A Rho-associated kinase inhibitor, Y-27632, has been suggested to inhibit the migration and metastasis of BCss [37]. Therefore, it can be inferred that the Rho/ROCK pathway inactivation is possibly implicated in the miR-381/BMI1-mediated events.

Conclusion

To sum up, the present study evidenced that miR-381 could inhibit BCs progression, presenting as decreased cell proliferation, migration, invasion and resistance to death, as well as tumor growth *in vivo*. BMI1 is a target mRNA of miR-381 and its down-regulation is, at least partially, implicated in the miR-381-mediated tumor suppressing roles. The current study also suggested that the Rho/ROCK pathway was activated following BMI1 activation, indicating its potential implication in BMI1-induced cell growth and metastasis. However, the exact role of this pathway, and if it abrogates the effect of miR-381 in BCs, were not included in the current study. Anyway, the paper may provide novel insights into gene-based BCs treatment. We hope more studies will be carried to validate our findings and to provide more understanding in BCs control.

Abbreviations

ANOVA, analysis of variance; BMI1, B-Cell-specific Moloney murine leukemia virus insertion region 1; CCK-8, cell counting kit-8; EMT, epithelial-mesenchymal transition; FBS, fetal bovine serum; FITC, fluorescein isothiocyanate; mean ± SD, mean ± standard deviation; MIBD, muscle invasive bladder cancer; miRNA, microRNA; NMIBD, non-muscle invasive bladder cancer; PBS, phosphate buffer saline; PI, propidium iodide; RT-qPCR, reverse transcription quantitative polymerase chain reaction; TNM, Tumor-Node-Metastasis; 3’UTR, 3’untranslated region.

Declarations

Ethics approval and consent to participate

This study was performed with the permission of the Clinical Ethical Committee of the First Affiliated Hospital of Jiamusi University. Signed informed consent was collected from each eligible participant. All

experimental procedures were conducted in line with the ethical guidelines for the study of experimental pain in conscious animals. Great attempts were made to minimize the number and suffering of animals.

Consent for publication

Not applicable.

Availability of data and materials

All the data generated or analyzed during this study are included in this published article. And the identifying/confidential patient data are not be shared.

Competing interests

The authors declare that they have no competing interests.

Funding

Not applicable.

Authors' contributions

DYC, LC proposed the protocol. DYC, LC, HFC, WSL were involved in data collection and management. HFC, WSL analyzed the data. DYC, LC contributed to manuscript writing and critically revised the manuscript. All authors read and approved the final manuscript.

Acknowledgements

Not applicable.

References

1. Siegel RL, Miller KD, Jemal A. Cancer statistics, 2020. CA Cancer J Clin. 2020;70(1):7–30.
2. Fernandez MI, Brausi M, Clark PE, Cookson MS, Grossman HB, Khochikar M, et al. Epidemiology, prevention, screening, diagnosis, and evaluation: update of the ICUD-SIU joint consultation on bladder cancer. World J Urol. 2019;37(1):3–13.
3. Crabb SJ, Douglas J. The latest treatment options for bladder cancer. Br Med Bull. 2018;128(1):85–95.
4. Ringuette-Goulet C, Bolduc S, Pouliot F. Modeling human bladder cancer. World J Urol. 2018;36(11):1759–66.
5. Adams BD, Kasinski AL, Slack FJ. Aberrant regulation and function of microRNAs in cancer. Curr Biol. 2014;24(16):R762–76.

6. Iwakawa HO, Tomari Y. The Functions of MicroRNAs: mRNA Decay and Translational Repression. Trends Cell Biol. 2015;25(11):651–65.
7. Jin D, Guo J, Wu Y, Chen W, Du J, Yang L, et al. Metformin-repressed miR-381-YAP-snail axis activity disrupts NSCLC growth and metastasis. J Exp Clin Cancer Res. 2020;39(1):6.
8. Xie Y, Qi J, Zhu C, Zhao D, Liao G. MiR-381 functions as a tumor suppressor in gastric cancer by targeting ROCK2. Int J Clin Exp Pathol. 2019;12(1):164–72.
9. Li J, Ying Y, Xie H, Jin K, Yan H, Wang S, et al. Dual regulatory role of CCNA2 in modulating CDK6 and MET-mediated cell-cycle pathway and EMT progression is blocked by miR-381-3p in bladder cancer. FASEB J 2019, 33(1):1374–1388.
10. M JR. S V. BMI1 and PTEN are key determinants of breast cancer therapy: A plausible therapeutic target in breast cancer. Gene. 2018;678:302–11.
11. Fu S, Luan T, Jiang C, Huang Y, Li N, Wang H, et al. miR-3622a promotes proliferation and invasion of bladder cancer cells by downregulating LASS2. Gene. 2019;701:23–31.
12. Tang W, Zhou W, Xiang L, Wu X, Zhang P, Wang J, et al. The p300/YY1/miR-500a-5p/HDAC2 signalling axis regulates cell proliferation in human colorectal cancer. Nat Commun. 2019;10(1):663.
13. Jiang C, Zhu W, Xu J, Wang B, Hou W, Zhang R, et al. MicroRNA-26a negatively regulates toll-like receptor 3 expression of rat macrophages and ameliorates pristane induced arthritis in rats. Arthritis Res Ther. 2014;16(1):R9.
14. Fankhauser CD, Mostafid H. Prevention of bladder cancer incidence and recurrence: nutrition and lifestyle. Curr Opin Urol. 2018;28(1):88–92.
15. Flannery K, Cao X, He J, Zhong Y, Shah AY, Kamat AM. Survival Rates and Health Care Costs for Patients With Advanced Bladder Cancer Treated and Untreated With Chemotherapy. Clin Genitourin Cancer. 2018;16(4):e909–17.
16. Usuba W, Urabe F, Yamamoto Y, Matsuzaki J, Sasaki H, Ichikawa M, et al. Circulating miRNA panels for specific and early detection in bladder cancer. Cancer Sci. 2019;110(1):408–19.
17. Enokida H, Yoshino H, Matsushita R, Nakagawa M. The role of microRNAs in bladder cancer. Investig Clin Urol. 2016;57(Suppl 1):60–76.
18. Tolle A, Jung M, Rabenhorst S, Kilic E, Jung K, Weikert S. Identification of microRNAs in blood and urine as tumour markers for the detection of urinary bladder cancer. Oncol Rep. 2013;30(4):1949–56.
19. Xiao S, Wang J, Xiao N. MicroRNAs as noninvasive biomarkers in bladder cancer detection: a diagnostic meta-analysis based on qRT-PCR data. Int J Biol Markers. 2016;31(3):e276–85.
20. Blanca A, Cheng L, Montironi R, Moch H, Massari F, Fiorentino M, et al. Mirna Expression in Bladder Cancer and Their Potential Role in Clinical Practice. Curr Drug Metab 2017, 18(8):712–722.
21. Ying Y, Li J, Xie H, Yan H, Jin K, He L, et al. CCND1, NOP14 and DNMT3B are involved in miR-502-5p-mediated inhibition of cell migration and proliferation in bladder cancer. Cell Prolif. 2020;53(2):e12751.

22. Wang JR, Liu B, Zhou L, Huang YX. MicroRNA-124-3p suppresses cell migration and invasion by targeting ITGA3 signaling in bladder cancer. Cancer Biomark. 2019;24(2):159–72.
23. Na XY, Shang XS, Zhao Y, Ren PP, Hu XQ. MiR-203a functions as a tumor suppressor in bladder cancer by targeting SIX4. Neoplasma. 2019;66(2):211–21.
24. Dou D, Ge X, Wang X, Xu X, Zhang Z, Seng J, et al. EZH2 Contributes To Cisplatin Resistance In Breast Cancer By Epigenetically Suppressing miR-381 Expression. Onco Targets Ther. 2019;12:9627–37.
25. Mi H, Wang X, Wang F, Li L, Zhu M, Wang N, et al. SNHG15 Contributes To Cisplatin Resistance In Breast Cancer Through Sponging miR-381. Onco Targets Ther. 2020;13:657–66.
26. Yi D, Xu L, Wang R, Lu X, Sang J. miR-381 overcomes cisplatin resistance in breast cancer by targeting MDR1. Cell Biol Int. 2019;43(1):12–21.
27. Shang A, Zhou C, Bian G, Chen W, Lu W, Wang W, et al. miR-381-3p restrains cervical cancer progression by downregulating FGF7. J Cell Biochem. 2019;120(1):778–89.
28. Hu J, Wu X, Yang C, Rashid K, Ma C, Hu M, et al. Anticancer effect of icaritin on prostate cancer via regulating miR-381-3p and its target gene UBE2C. Cancer Med. 2019;8(18):7833–45.
29. Siddique HR, Saleem M. Role of BMI1, a stem cell factor, in cancer recurrence and chemoresistance: preclinical and clinical evidences. Stem Cells. 2012;30(3):372–8.
30. Ren H, Du P, Ge Z, Jin Y, Ding D, Liu X, et al. TWIST1 and BMI1 in Cancer Metastasis and Chemoresistance. J Cancer. 2016;7(9):1074–80.
31. Wu KJ, Yang MH. Epithelial-mesenchymal transition and cancer stemness: the Twist1-Bmi1 connection. Biosci Rep 2011, 31(6):449–455.
32. Kim M, Lee S, Park WH, Suh DH, Kim K, Kim YB, et al. Silencing Bmi1 expression suppresses cancer stemness and enhances chemosensitivity in endometrial cancer cells. Biomed Pharmacother. 2018;108:584–9.
33. Li J, Vangundy Z, Poi M. PTC209, a Specific Inhibitor of BMI1, Promotes Cell Cycle Arrest and Apoptosis in Cervical Cancer Cell Lines. Anticancer Res. 2020;40(1):133–41.
34. Luo H, Yang R, Li C, Tong Y, Fan L, Liu X, et al. MicroRNA-139-5p inhibits bladder cancer proliferation and self-renewal by targeting the Bmi1 oncogene. Tumour Biol. 2017;39(7):1010428317718414.
35. Liu L, Qiu M, Tan G, Liang Z, Qin Y, Chen L, et al. miR-200c inhibits invasion, migration and proliferation of bladder cancer cells through down-regulation of BMI-1 and E2F3. J Transl Med. 2014;12:305.
36. Tang Y, He Y, Zhang P, Wang J, Fan C, Yang L, et al. LncRNAs regulate the cytoskeleton and related Rho/ROCK signaling in cancer metastasis. Mol Cancer. 2018;17(1):77.
37. Jiang L, Wen J, Luo W. Rhoassociated kinase inhibitor, Y27632, inhibits the invasion and proliferation of T24 and 5367 bladder cancer cells. Mol Med Rep. 2015;12(5):7526–30.
38. Legends.

Figures

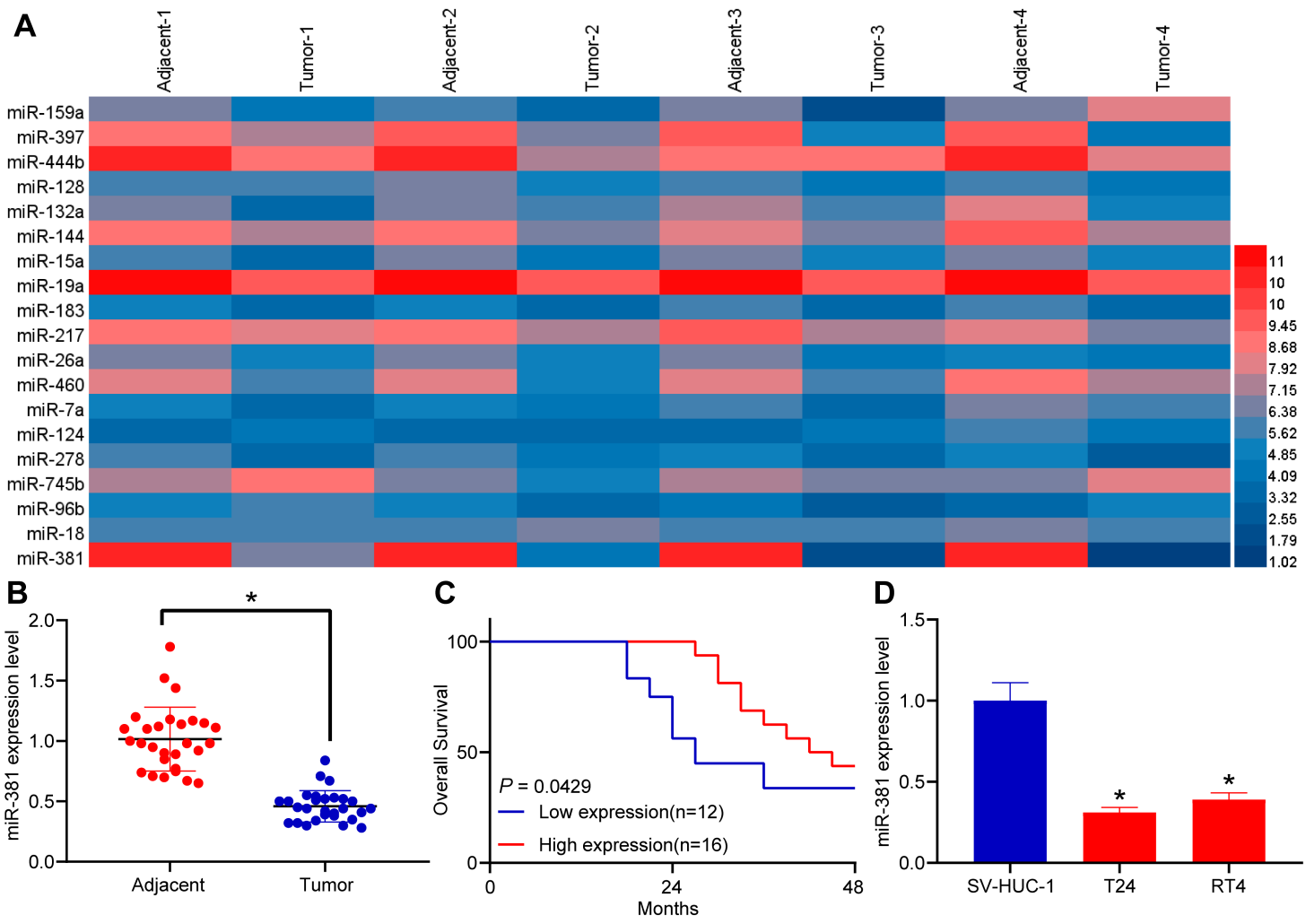

Figure 1

Poor miR-381 expression in BCs patients indicates unfavorable prognosis. A, differentially expressed miRNAs between BCs tissues and the paired adjacent tissues determined by microarray analysis ($p < 0.05$, $|logFC| \geq 1.5$); B, miR-381 expression in the BCs and paired adjacent tissues determined by RT-qPCR (*$p < 0.05$, two-way ANOVA); C, survival analysis of BCs patients with different level of miR-381; D, miR-381 expression in BCs cells (T24 and RT4) and in normal bladder epithelial cell line SV-HUC-1 determined by RT-qPCR (*$p < 0.05$, one-way ANOVA); Repetition = 3.

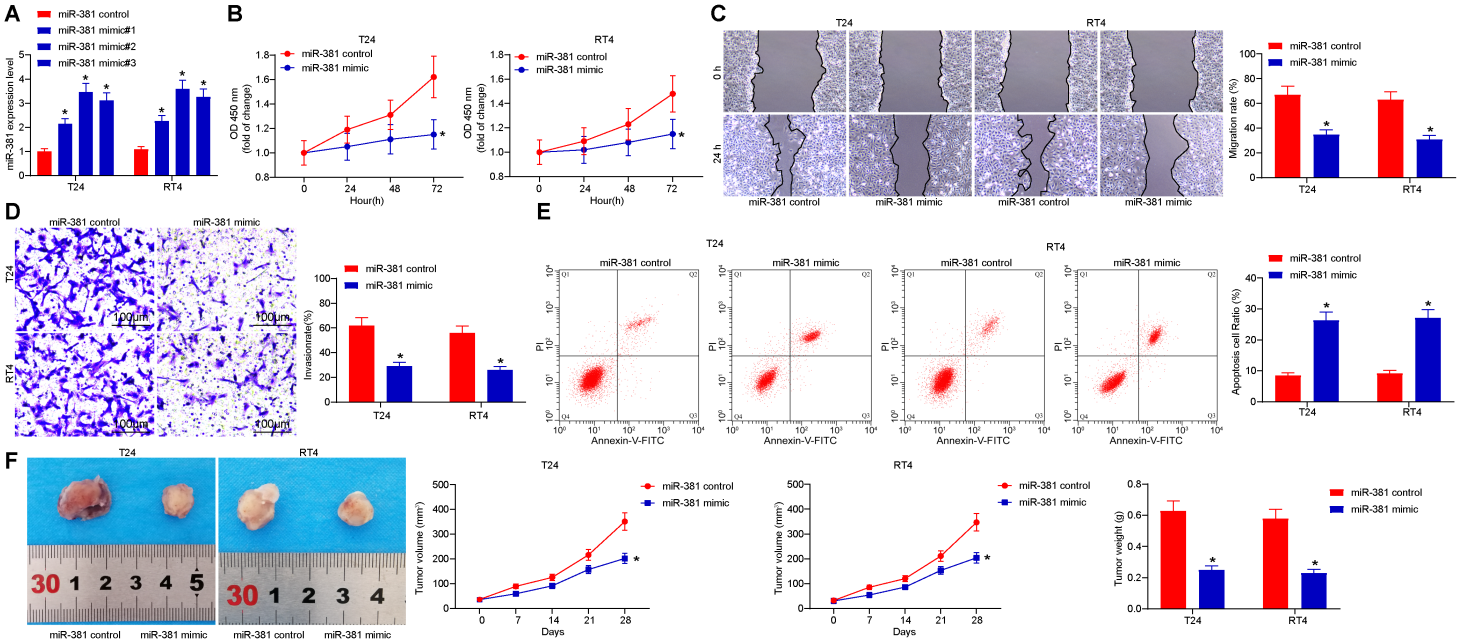

Figure 2

miR-381 inhibits malignant behaviors of BCs cells. A, miR-381 expression in cells after miR-381 mimic transfection detected by RT-qPCR, and it was found that miR-381 mimic#2 showed the best efficacy (*p < 0.05, two-way ANOVA); B, optical density at 450 nm measured by two-way ANOVA (*p < 0.05, two-way ANOVA); C, migration rate of each group of cells at the 24th hour (*p < 0.05, two-way ANOVA); D, invasion rate of each group of cells measured by Transwell assay (*p < 0.05, two-way ANOVA); E, apoptosis rate of cells determined by flow cytometry (*p < 0.05, two-way ANOVA); F, tumor volume change and weight on the 28th day after implantation of cells transfected miR-381 mimic (*p < 0.05, two-way ANOVA); Repetition = 3.

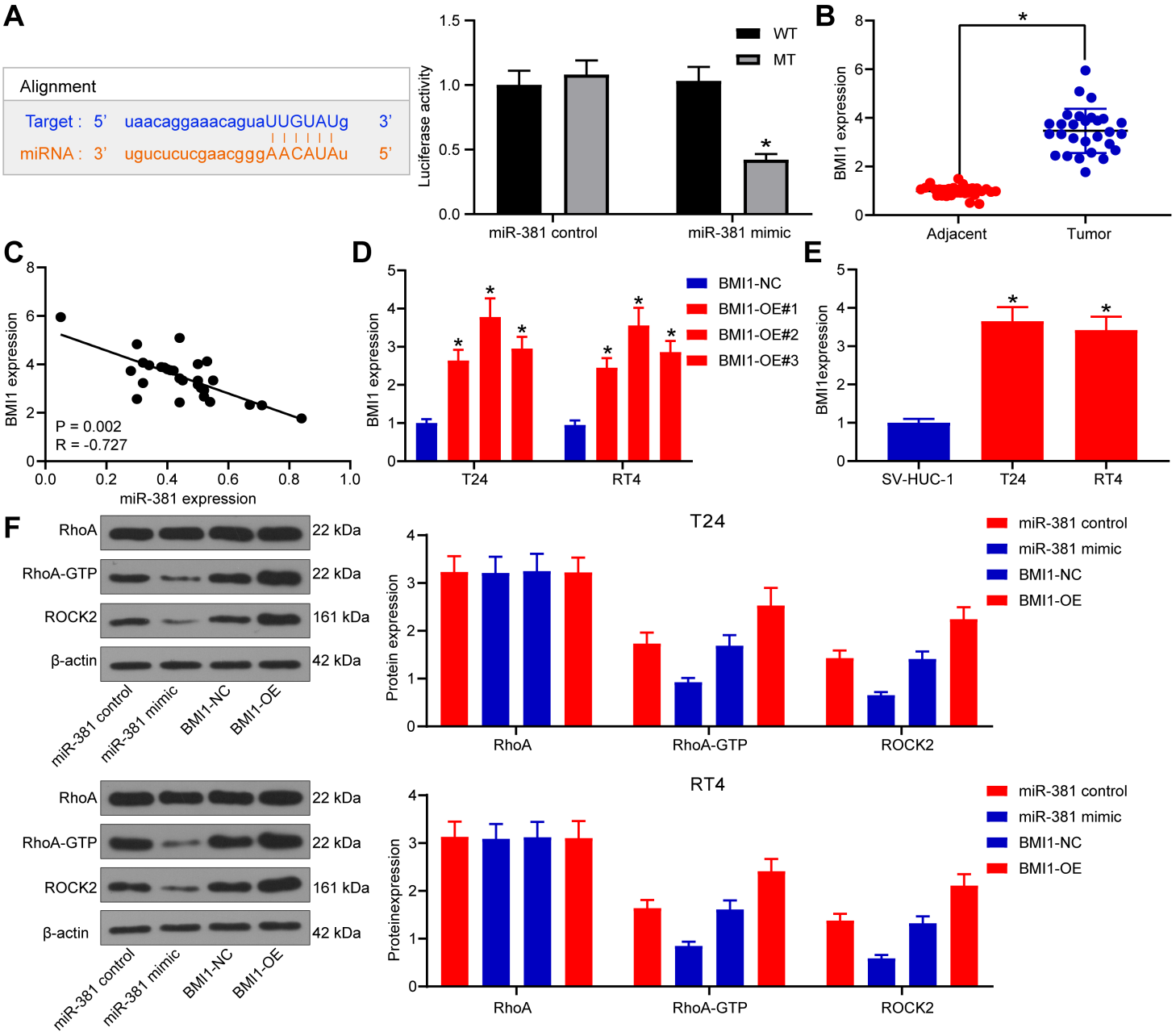

Figure 3

miR-381 targets BMI1 to inactivate the Rho/Rock pathway. A, target relationship between miR-381 and BMI1 predicted on StarBase (http://starbase.sysu.edu.cn/) and validated through a dual luciferase reporter assay (*p < 0.05, two-way ANOVA); B, BMI1 expression in BCs tissues determined by RT-qPCR (*p < 0.05, two-way test); C, BMI expression in BCs cell lines (T24 and RT4) and in normal bladder epithelial cells determined by RT-qPCR (*p < 0.05, one-way ANOVA); D, correlation analysis between miR-381 and BMI1 expression in BCs tumor tissues; E, BMI1 expression in BCs tumor tissues after BMI1-OE vector transfection detected by RT-qPCR (*p < 0.05, two-way ANOVA). F, protein levels of RhoA and ROCK2 in each group of cells measured by western blot analysis (*p < 0.05, two-way ANOVA); Repetition = 3.

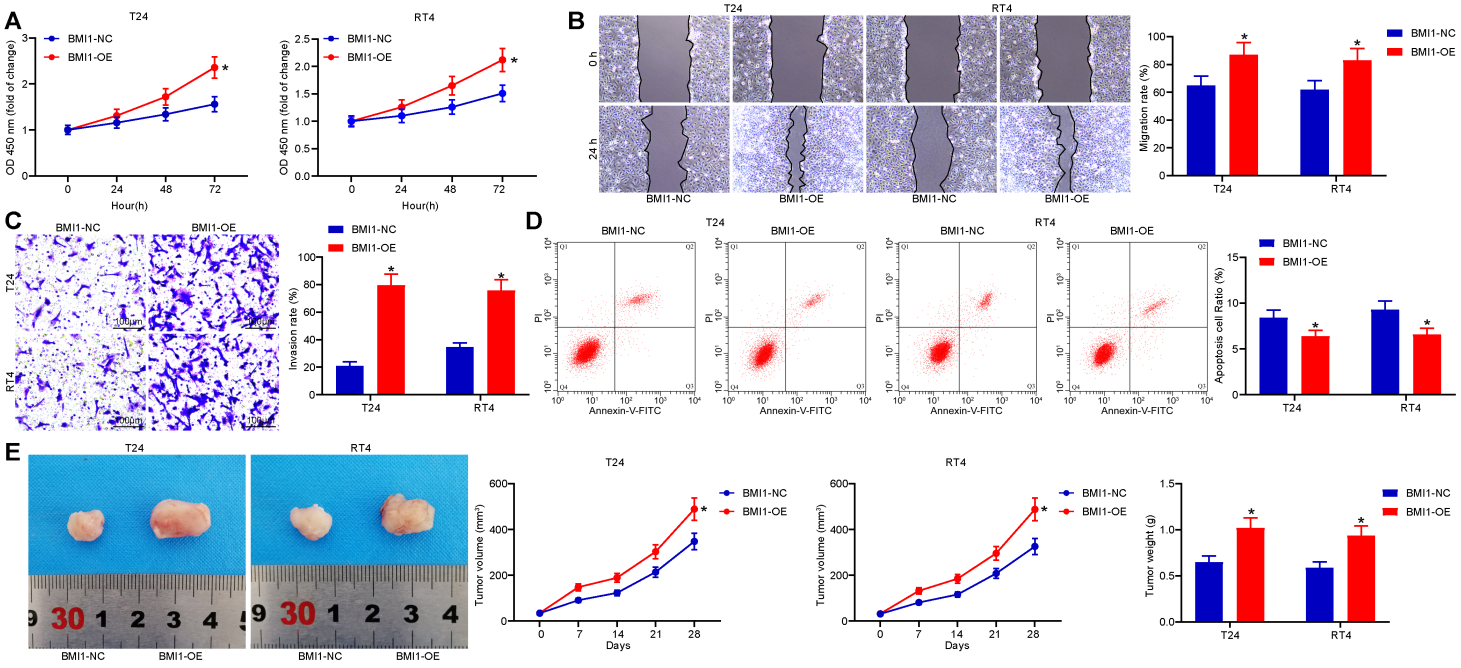

Figure 4

Overexpression of BMI1 promotes BCs progression. A, optical density at 450 nm of each group of cells according the CCK-8 method (*p < 0.05, two-way ANOVA); B, migration distance at the 24th hour measured by the scratch test (*p < 0.05, two-way ANOVA); C, number of invaded cells at the 24th hour determined by the transwell assay (*p < 0.05, two-way ANOVA); D, number of PI-Annexin V-double positive cells detected by flow cytometry (*p < 0.05, two-way ANOVA); E, tumor growth rate change and weight on the 28th day in nude mice (n = 8) (*p < 0.05, two-way ANOVA); Repetition = 3.

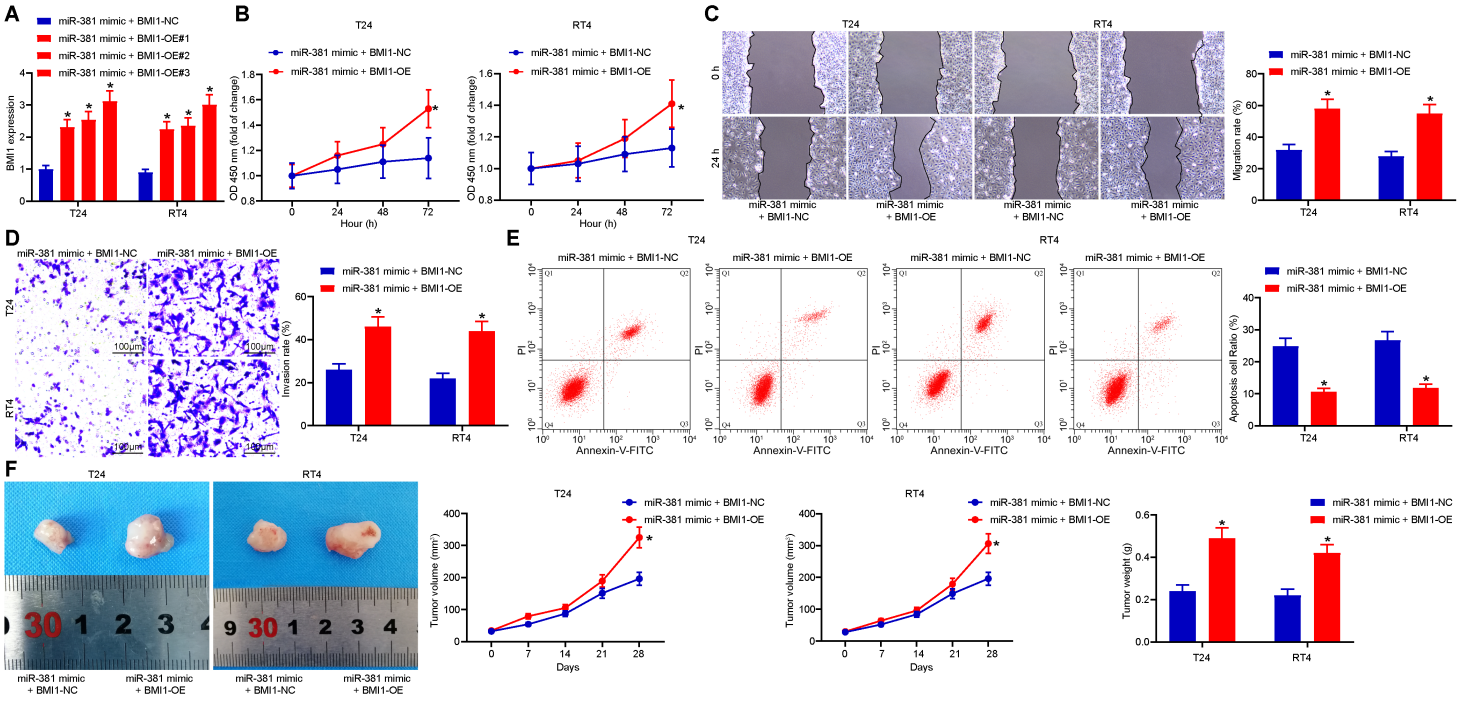

Figure 5

BMI1 partially blocks the role of miR-381. A, cells pre-transfected with miR-381 mimic were further transfected with BMI1-OE vectors, and it was found that BMI1-OE#3 presented the best overexpressing efficiency (*p < 0.05, two-way ANOVA); B, optical density at 450 nm of each group of cells according the CCK-8 method (*p < 0.05, two-way ANOVA); C, migration distance at the 24th hour measured by the scratch test (*p < 0.05, two-way ANOVA); D, number of invaded cells at the 24th hour determined by the transwell assay (*p < 0.05, two-way ANOVA); E, number of PI-Annexin V-double positive cells detected by flow cytometry (*p < 0.05, two-way ANOVA); F, tumor growth rate change and weight on the 28th day in nude mice (n = 8) (*p < 0.05, two-way ANOVA); Repetition = 3.

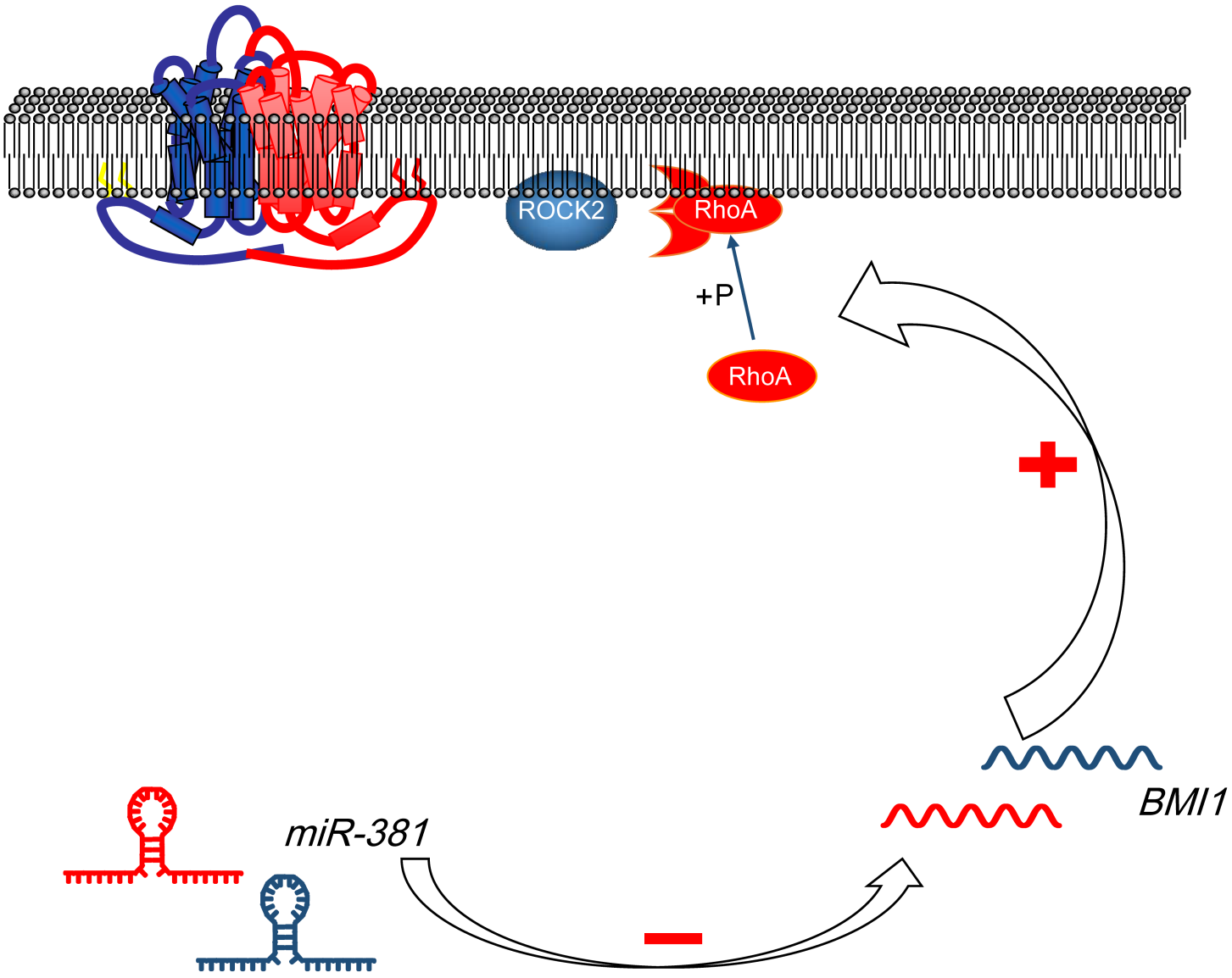

Figure 6

Diagram for the molecular mechanism. In BCs cells, miRNA-381 directly binds to BMI1 expression to inhibit RhoA phosphorylation and ROCK2 expression, leading to suppressed malignant behaviors of bladder cells.

Supplementary Files

This is a list of supplementary files associated with this preprint. Click to download.

- ARRIVEChecklist.docx